DEVELOPEMENT AND CHARACTERIZATION OF CHROMIUM COATING DEPOSITED ON ZIRCALOY-4 SUBSTRATE

DEZVOLTAREA ȘI CARACTERIZAREA UNOR ACOPERIRI DE CROM DEPUSE PE SUBSTRAT DE ZIRCALOY-4

Diana DINIAȘI[1], Alexandru ANGHEL[2], Valentina ROȘU[1], Vlăduț ION[1], Aurel DAVID[1]

Abstract: *A Cr layer of approximately 500 nm thickness has been deposited on Zy-4 alloy using thermionic vacuum arc (TVA) method. The coating microstructure and morphology have been investigated using specific analysis techniques (X-Ray Diffraction, Scanning Electron Microscopy and X- ray Photoelectron Spectroscopy). To assess the protective character of the metallic Cr coating, electrochemical measurements have been performed. The higher values of impedance and phase angle obtained for the coated Zy-4 sample indicates a protective character of the metallic Cr layer. In the same time, results obtained from the potentiodynamic polarization tests, showed a better corrosion behaviour of coated Zy-4 sample than uncoated sample. All the applied methods indicate an improving of the corrosion behaviour of Zy-4 alloy after coating with thin metallic Cr layer.*

Keywords: Chromium coated Zy-4, XRD, XPS, SEM, EIS

Rezumat: *Utilizând medoda arcului termoionic în vid (TVA) a fost depus un strat de crom, de aproximatix 500 nm pe un substrat de Zy-4. Microstructura și morfologia acoperirii au fost investigate utilizând difracția de raze, microscopia electronica și spectroscopia fotoelectronilor de raze X. Pentru evaluarea caracterului protector al acoperirii au fost realizate măsurători electrochimice. Valorile mari ale impedanței și unghiului de fază au indicat un caracter protector al acoperirii realizate. Acest lucru este confirmat și de rezultatele obținute în urma aplicării testelor de polarizare potențiodinamică liniară. Toate metodele folosite în caracterizarea acoperirii indică o îmbunătățire a comportării la coroziune a aliajului Zy-4 acoperit cu crom metalic.*

Cuvinte cheie: Zy-4 acoperit cu crom, XRD, XPS, SEM, EIS

[1] Institute for Nuclear Research, Pitesti, Romania, diana.diniasi@nuclear.ro
[2]National Institute for Laser, Plasma and Radiation Physics, Măgurele, Romania

1. Introduction

Owing to their corrosion resistance, irradiation resistance, good ductility and low neutron absorption cross section the zirconium based alloys, like Zircaloy-2 (Zy-2) and Zircaloy-4 (Zy-4) has been used as fuel cladding materials since 1950 [1], [2]. However, the Three Mile Island (1979) and Fukushima Daiichi (2011) events led to a worldwide interest in development of fuels with enhanced performance during such rare events [3], [4]. In response, accident tolerant fuel (ATF) development programs were started in many research institutions and industry teams [4], [5]. The research investigations are focused on three main directions [6], [7]:

- enhanced of both chemical composition and technology fabrication process for Zr alloys leading to advanced materials: E635, ZIRLO, M5, MDA, HiFi, X5A, etc. [8].
- development of advanced alloys suitable for use in special event The ATF new candidate materials, for replacements of current Zr include refractory metal, advanced steels or SiC/SiC [9].
- development of new advanced coating on existing alloys such as Zircaloy 4 which seems to be the most investigated direction since no major change in design changes of LWR required and is the most economic strategy [10] - [14].

The aim of development of protective coatings on zirconium alloys is to increase the corrosion resistance, which is the main cause on limiting the fuel burnup extension. According to the technical documentation have been proposed various materials for covering the zirconium alloys, with thicknesses of 0.0215-250 μm [15], by various techniques. Up to the moment the coatings can be divided as: metallic/non-metallic/ceramic (oxides, nitrates, carbides)/composite/multilayer coatings.

The main advantages and challenges regarding the development of coated zirconium fuel cladding are as follows [14], [16]:

- ✓ developing coatings with desired microstructure on the full-length cladding tube;
- ✓ relatively low fabrication temperature to avoid changes in the material structure;
- ✓ low neutronic penalty if coating is sufficiently thin (<20 μm);
- ✓ good thermal properties (such as thermal conductivity and stability, comparable thermal expansion coefficients and melting temperature);
- ✓ good corrosion and irradiation resistance under normal operation conditions;

- ✓ good mechanical properties (wear, fracture, spallation, and fretting-corrosion resistance) under normal and accident conditions;
- ✓ good adherence and ductility to sustain high viscoplastic deformation of Zr-based cladding in case of clad ballooning during accidental conditions;
- ✓ Improved resistance to high-temperature steam or air under accident conditions.

Oxidation resistant coatings are an attractive and short term solution to enhance the resistance of current zirconium based nuclear fuel cladding to accelerated high temperature (HT) steam oxidation (and potentially hydriding) upon accidental scenario such as loss-of-coolant accident (LOCA) [17].

The general coating techniques include physical vapor deposition (PVD), chemical vapor deposition (CVD), electrodeposition, thermal spray, cold spray, and pack cementation [18]. The techniques can be modified and, in some cases, combined, to develop coatings with desired properties.

The coated zirconium alloys have been largely investigated [19] - [22] regarding the coating methods and deposition parameters, microstructure, coating thickness, oxidation and corrosion behaviour. In general, it was concluded that regarding corrosion resistance and neutron stability the Cr and CrN coatings are the most promising. Both types of coatings are resistant to corrosion in LWR coolant and stable under neutron irradiation at expected temperatures, but Cr-coatings provide increased resistance to high temperature steam oxidation as well, while CrN does not [23].

Thermionic Vacuum Arc (TVA) technique is a combination of evaporation by electron bombardment and anodic arc. The basic principle of TVA is ignition of an arc plasma in the vapors of the material of interest. The films obtained using TVA plasma are very adherent, compact, smooth, pure and pore free.

The aim of this paper is the characterization and the assessment of corrosion behaviour of Cr coating deposited on Zy-4 alloy by TVA.

2. Experimental

2.1. Materials

The Zircaloy-4 tube (Table 1) with an outer diameter of 13 mm and a wall thickness of 0.45 mm was cut into 20 mm sections and then halved lengthwise. Before the TVA, the substrates were ultrasonicated in isopropyl alcohol for 15 minutes, followed by nitrogen drying.

The selection of coating material was based on the neutron cross-section, thermal conductivity, thermal expansion, melting point, phase transformation behaviour, and high-temperature oxidation resistance. Cr pellets of 99.99% purity and 1-3 mm dimensions were selected for coating the surface of Zy-4 alloy.

Table 1. **Composition of Zircaloy-4 alloy (%)**

Alloying Elements, [wt.%]				
Sn	Fe	Cr	O	Zr
1.32	0.29	0.14	0.12	Balance

Cr coatings studied in this paper have been deposited using TVA technique. The equipment has been developed by Laboratory of Low Temperature Plasma from National Institute for Laser, Plasma&Radiation **Physics (NILPRP).**

2.2. Characterization methods

Microstructure and the properties of the coating depends on the materials used for deposition, the process parameters and the coating thickness. For a complete characterization, have been identified: coating elemental composition, coating thickness, uniformity and roughness, the eventually presence of cracks/pores and coating structural characteristics.

For the morphological characterization scanning electron microscopy (SEM, Hitachi SU 8230 scanning electron microscope) at a pressure of 0.7 torr at 10 and/or 15kV were used. To identify the elemental composition of the samples an energy dispersive spectra detector (EDS) which was used.

The XRD patterns of the investigated samples were obtained using a D8 ADVANCE (Brucker-ASX) X-ray Diffractometer in a θ-2θ geometry using CuKα radiation (λ= 1.5406Å) and operating at room temperature. X-ray diffraction measurements of all the samples were carried out in the 5–140° range. The identification of the phase was made by referring to the International Center for Diffraction Data—ICDD (PDF-2) database.

XPS measurements were performed on chromium coated Zy-4 alloys using an ESCALAB XI+ X-ray Photoelectron Spectrometer (XPS) Microprobe. Monochromatic Al Kα radiation (1486.6 eV) and 900 μm X-ray spot size was used. The acquired spectra were calibrated with respect to the C1s line of surface adventitious carbon at 284.8 eV. An electron flood gun was used to compensate for the charging effect in insulating samples.

2D roughness profile was measured by Mitutoyo SURFTEST SJ-210 profilometer, with a measuring range up to 360 μm.

An electrochemical measurement system PARSTAT 2273 (Princeton Applied Research, AMETEK, OakRidge, TN, USA) was used to perform all electrochemical measurements. Also, a classical three-electrode electrochemical cell consisting of a working electrode, a saturated calomel reference electrode (SCE) and two auxiliary electrodes (graphite rods) was used to perform electrochemical measurements. All electrochemical tests were performed at room temperature (22 ± 2 °C). The electrochemical methods used were: open circuit potential variation, electrochemical impedance spectroscopy and potentiodynamic measurements.

Electrochemical impedance spectroscopy (EIS) tests were performed in a chemically inert solution with pH = 7.26 (0.05 M boric acid with 0.001 M borax solution), at open circuit potential (OCP) with an amplitude of 10 mV in the frequency range from 100 mHz to 100 kHz after OCP stabilization.

Potentiodynamic measurements were made in LiOH solution at pH 10.5 with a scan rate of 1 $mV \cdot s^{-1}$ and a range from −250 to 1000 mV relative to the open current potential (OCP).

3. Results and discussions

3.1. Scanning electron microscopy measurements

The thickness and elemental composition of the chromium coating have been investigated by SEM and EDS analysis. Also, the eventual presence of defects and pores has been studied.

In Fig.1 are presented the SEM cross sections and the EDS profile of Cr coating.

The presence of a uniform layer with an average thickness of 500 nm can be observed in Fig.1 a). The chromium layer presents a columnar structure with a small number of fine cannelures (indicated by the white arrows), without any others visible defects. The EDS analysis revealed the increase of Cr content simultaneously with the decrease of Zr content, starting from the base metal through the surface of the material.

3.2. XRD Measurements

The XRD analysis results for uncoated (blue line) and coated (red line) Zy-4 samples are shown in Fig. 2. The appearance of a crystalline phase of Chromium with a preferred orientation (110) can be observed.

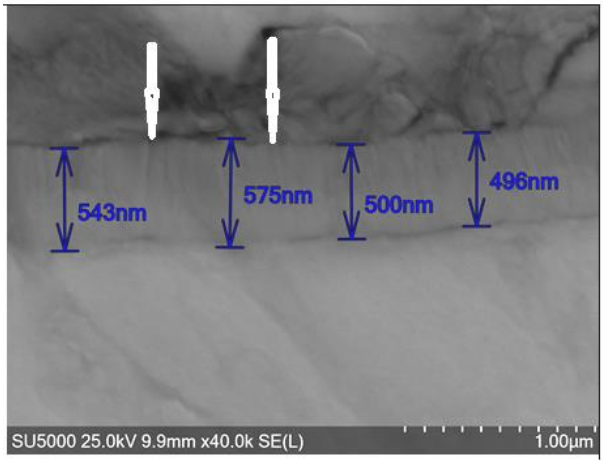

a)

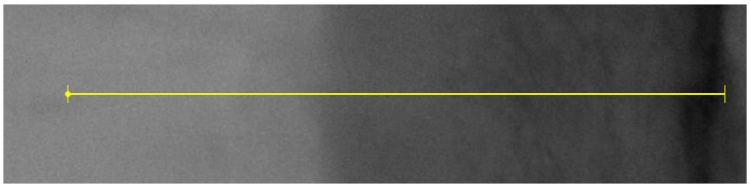

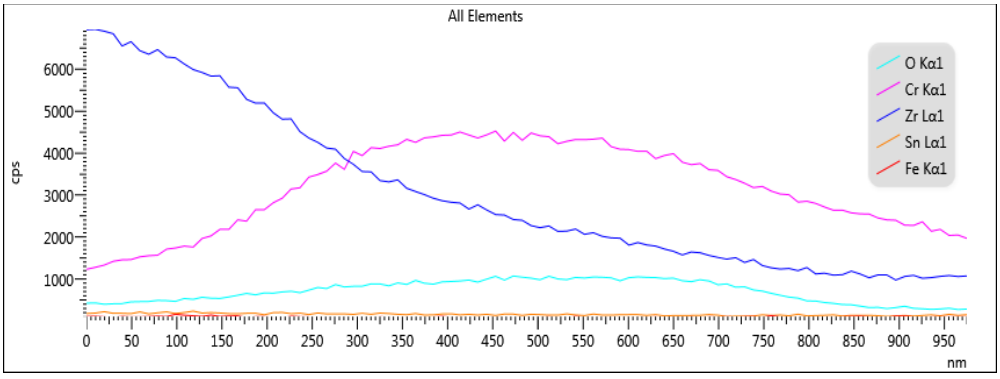

b)

Figure 1. a) SEM cross section micrographs for Cr coated Zy-4 and b) EDS profile of chromium coating.

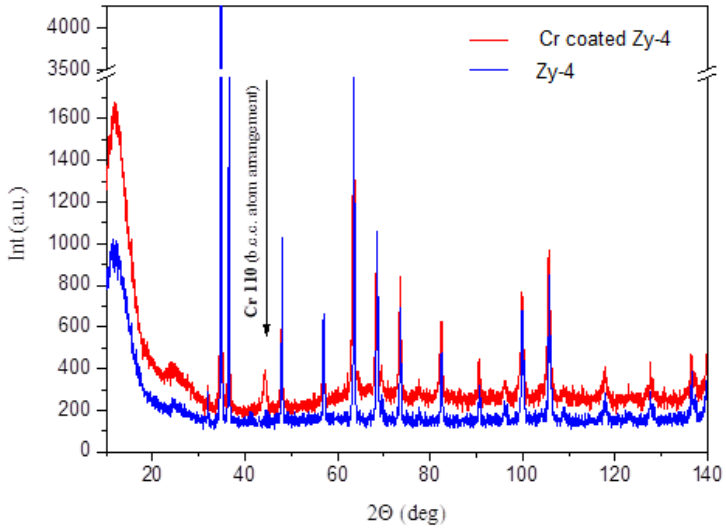

Figure 2. XRD diffractograms of uncoated and Cr coated Zy-4 samples .

3.3. XPS analysis

The XPS measurements were performed to obtain information about surface chemistry and oxidation states of the detected elements.

Fig. 3 a) shows a decreasing graphitic contribution with the increase of the carbide feature after cleaning the surface by Ar^+ ion sputtering. After deconvoluting the C1s photoelectron line, we can notice the chemical species labeled on the spectrum (Fig. 3 b)): oxidized carbon, C-C chemical bonding and carbides.

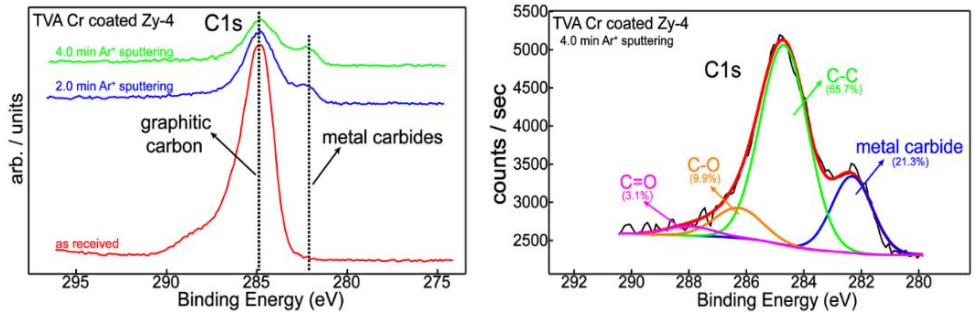

a) b)

Figure 3. a) C1s XPS superimposed spectra before and after Ar^+ ion sputtering; b) C1s XPS deconvoluted spectrum after 4.0 min Ar^+ ion sputtering.

For a general overview of the chromium chemical behavior, the spectra were selected and superimposed before and after sputtering (Fig. 4 a)). It can be seen that a dominant metallic contribution appears after 2.0 and 4.0 min Ar^+ ion sputtering assessed by peak binding energy and line shape asymmetry. In the "as received" stage (before Ar^+ ion sputtering), a mixture of oxidized and metallic chromium was detected.

The spectral deconvolution of $Cr2p_{3/2}$ line was performed, in order to distinguish chromium chemical states (Fig. 4 b)). Therefore, Cr^0 (metallic), Cr^{3+} (Cr_2O_3) and Cr^{6+} (CrO_3) oxidation states together with chromium nitride were labeled on the spectrum. After 4.0 min Ar^+ ion sputtering, the XPS signal was collected from the subsurface region, indicating an enriched metallic contribution (~75%), although a chemical interaction between nitrogen and chromium can be noticed.

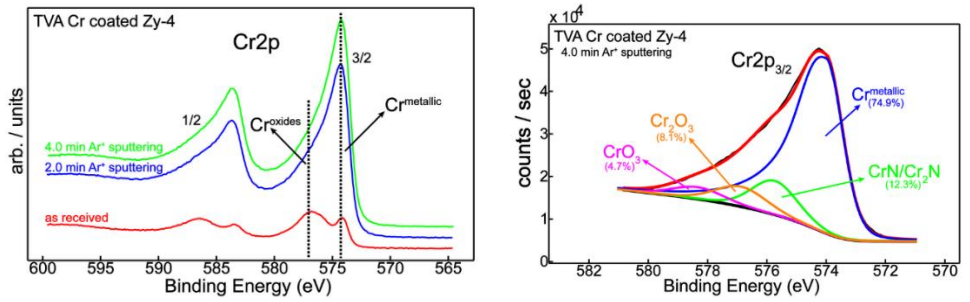

a) b)

Figure 4. a) Cr2p XPS superimposed spectra before and after Ar^+ ion sputtering; b) $Cr2p_{3/2}$ XPS deconvoluted spectrum after 4.0 min Ar^+ ion sputtering.

The quantitative analysis (Table 2) illustrates a decreasing trend for carbon and oxygen with an increasing nitrogen and chromium, from surface to subsurface region.

Table 2. **Element relative concentration (at. %)**

TVA Cr coated Zy-4	C1s	O1s	N1s	Cr2p
as received	56.4	31.7	2.4	9.5
2.0 minAr^+sputtering	22.5	25.4	12.5	39.6
4.0 minAr^+sputtering	14.2	23.3	16.5	46.0

The surface chemistry of nitrogen is in agreement with chromium chemistry. Therefore, the N1s superimposed spectra show the chemical

modification between surface and subsurface, from adsorbed nitrogen on the surface to nitrides (Fig. 5 a)). Additionally, this was accompanied by nitrogen concentration increase, from 2% to 16% (Table 2).

After peak-fitting the N1s signal (Fig. 5 b)), we can notice a dramatic decrease of chemisorbed nitrogen with an increase of chromium nitrides. The nitrides could be buried under carbon.

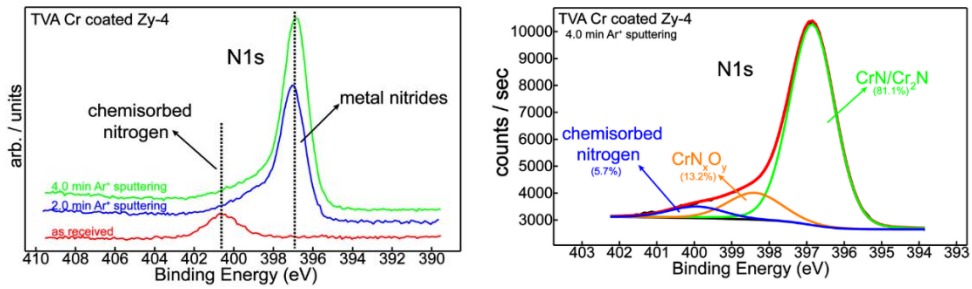

a) b)

Figure 5. a) N1s XPS superimposed spectra before and after Ar^+ ion sputtering; b) N1s XPS deconvoluted spectrum after 4.0 min Ar^+ ion sputtering.

3.4. Roughness measurements

Roughness measurements were performed on uncoated and Cr coated Zy-4 samples, and the obtained results are summarized in Table 3.

Table 3. **Average roughness values**

Sample	R_a (µm)	R_{max} (µm)	R_z (µm)
Zy-4	0.476	3.87	3.27
Zy-4 + Cr	0.358	3.94	3.23

R_a: arithmetical mean roughness
R_{max}: maximum roughness depth
R_z: maximum height of profile

R_a is the most frequently used parameter for roughness assessment. Therefore, we can observe a slightly roughness decrease for the coated sample compared to uncoated sample (from 0.476 to 0.358 µm). The surface of the studied material could not be metallographic prepared because of the sample complex geometry. Hence, the minor surface imperfections were filled after the deposition process resulting in a diminished roughness value.

3.5. Electrochemical characterization

3.5.1. Open circuit potential measurements

Following the curves trend, we can obtain qualitative information regarding the influence of temperature and testing environment on the chromium coating. Thus, in Fig. 6 we can observe that the corrosion potential of the coated sample starts from a higher value (-184 mV), than the corrosion potential for the uncoated sample (-530 mV). Also, Ecorr has a constant trend with time, meaning that the coating is continuous, stable and there are no reactions to the solution-substrate interface.

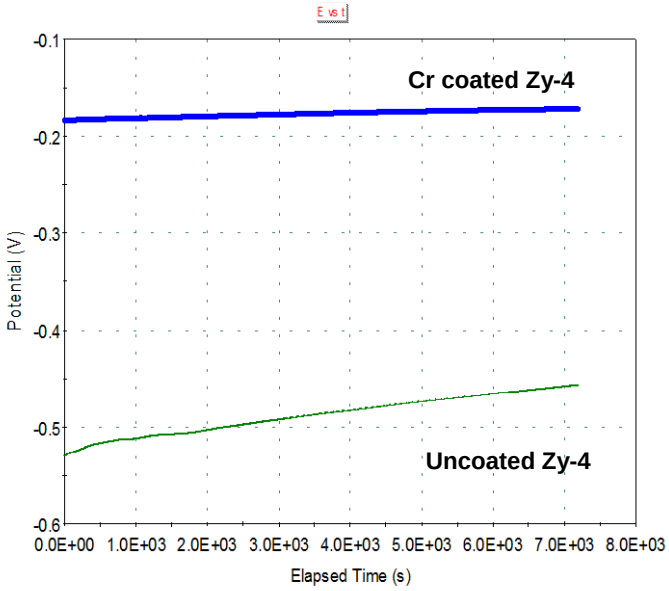

Figure 6. Superimposed OCP curves of uncoated Zy-4 and Cr coated Zy-4.

3.5.2. Potentiodynamic polarization tests

Regarding the behaviour of Cr coated Zy-4 in a specific primary circuit solution, the potentiodynamic polarization curves of the uncoated and coated samples were recorded and are presented in Figure 7.

The Tafel extrapolation method was applied on the polarization curves in order to obtain the kinetic parameters, which are shown in Table 4. The main parameters are the corrosion potential (Ecorr), corrosion rate (V_{corr}), corrosion current (i_{corr}) and polarization resistance (Rp).

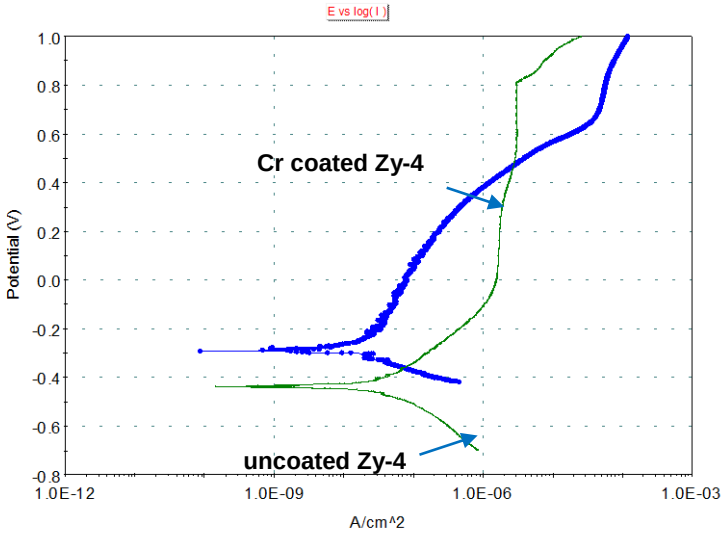

Figure 7. Superimposed polarization plots of uncoated and Cr coated Zy-4.

Table 4. **Polarizations parameters of uncoated and Cr coated Zy-4**

Sample	**E_{corr}, mV**	**i_{corr}, µA**	**V_{corr}, mm·year^{-1}**	**R_p (MΩ·cm^2)**
Uncoated Zy-4	-436	0.19	$6.17 \cdot 10^{-4}$	0.26
Cr coated Zy-4	- 288	0.11	$2.6 \cdot 10^{-4}$	0.28

As can be seen from Figure 7 and Table 4, for the Cr coated Zy-4 sample, lower values of corrosion current and corrosion rate were obtained compared to the uncoated sample. Also, a higher value of the polarization resistance of the coated sample was recorded and the Ecorr of the same sample has shifted to more electropositive values.

3.5.3. Electrochemical impedance spectroscopy

For a qualitative evaluation of the Cr coating protective properties, electrochemical impedance spectroscopy method has been used.

In Fig. 18 are presented the Bode and Nyquist diagrams, recorded at open circuit potential after 10 min of immersion in test solution.

From the Bode curves, we can see that Cr coated Zy-4 sample presents a higher impedance magnitude, |Z|, and a higher angle phase. The impedance values being directly proportional to oxide resistance we can say that this high value obtained for impedance modulus indicate a good corrosion resistance of

the coated sample. Also, the Nyquist curve is a regular semicircle, which denotes the fact that surface of the coating is uniform and smooth. For the coated sample, a higher value of the capacitive semicircle diameter was recorded compared to the uncoated sample.

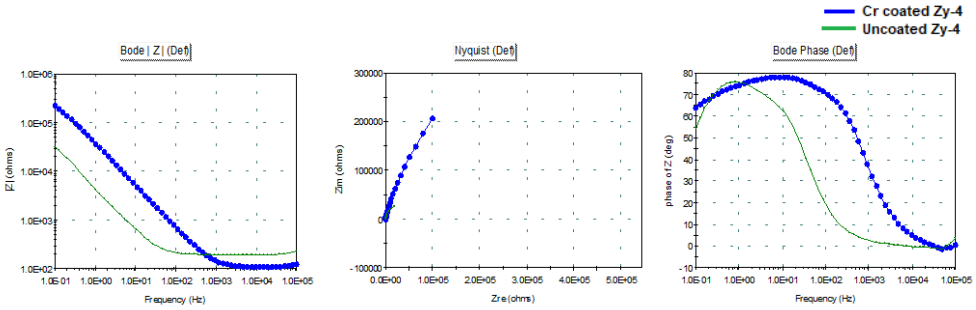

Figure 8. Superimposed impedance spectra of uncoated Zy-4 and Cr coated Zy-4.

In Fig. 9 are shown the Nyquist plots after application of Kramers-Kronig Transform for coated and uncoated Zy-4 samples. The overlap of the measured and calculated curves demonstrates the validity of the fittings and a higher polarization resistance (Rp) value has been obtained for the coated sample ($3 \cdot 10^6$ compared to $3.1 \cdot 10^5 \omega \cdot cm^2$).

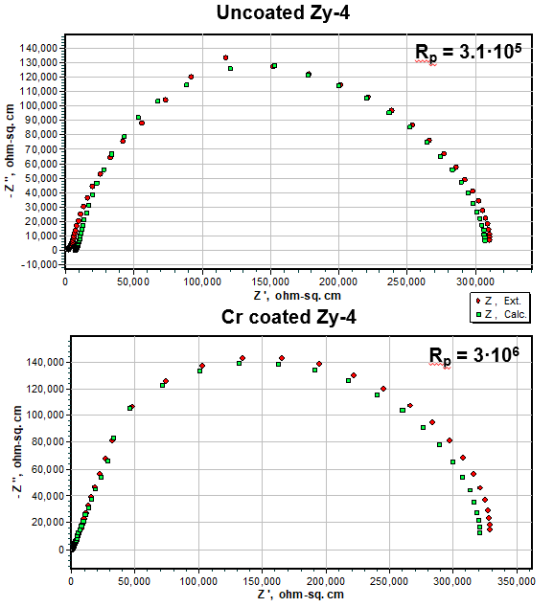

Figure 9. Nyquist plots after application of Kramers-Kronig Transform.

4. Conclusions

Metallic chromium has been successfully deposited on Zircaloy-4 substrate by thermionic vacuum arc method. The morphology and composition as well as the electrochemical properties of the coating have been evaluated by SEM, XRD, XPS and electrochemical measurements.

SEM measurements indicate the presence of an uniform coating, with an average thickness of 529 nm. The chromium layer presents a columnar structure with a small number of fine cannelures, without any others visible defects. The presence of chromium content has been highlighted by EDS analysis, noting a concentration increase from the base metal through the surface of the sample.

The roughness measurements have revealed a surface roughness decrease by 0.118 μm after applying the chromium coating on the Zy-4 substrate.

XRD analysis revealed the presence of a crystalline phase of Cr with a preferred orientation (110).

Information about surface chemistry and oxidation states of the detected elements has been obtained by XPS, confirming the presence of metallic chromium.

Qualitative information has been obtained by OPC measurements, therefore the corrosion potential of the coated sample placed towards a higher anodic value (-184 mV), than the corrosion potential of the uncoated sample (-530 mV), and also presented a constant evolution during the test.

Potentiodynamic polarization test indicates lower values of corrosion current density and corrosion rate for the coated sample compared to the uncoated sample. Furthermore, the coated sample presents a higher value of the polarization resistance.

Good corrosion properties of chromium coating were highlighted by EIS, confirmed by high values of impedance and angle phase.

REFERENCES

[1] *P. Cantowine et B. Rand*, "Irradiation Performance: Light Water Reactor Fuels in Encyclopedia of Nuclear Energy," Elsevier, Vol. 2, pag. 377-391, 2021.

[2] *H. Kim, J. Yang, W. Kim et Y. Koo*, "Development status of accident-tolerant fuel for light water reactors in Korea," Nuclear Engineering and Technology, Vol. 1, pag. 1-15, 2016.

[3] *M. Hirano, T. Yonomoto, M. Ishigaki, N. M. Y. Watanabe, Y. Sibamoto, T. Watanabe et K. Moriyama*, "Insights from review and analysis of the Fukushima Daiichi accident," Journal of Nuclear Science and Technology, Vol. 49, pag. 1–17, 2012.

[4] *F. Goldner*, "Development Strategy for advanced LWR Fuels with Enhanced Accident Tolerance," USDOE Office of Nuclear Energy, Washington, DC, USA, 2012.

[5] *U.S. Department of Energy*, "Development of Light Water Reactor Fuels with Enhanced Accident Tolerance – Report to Congress," Washington, DC, USA, April, 2015.

[6] *A. Sowder*, "Challenges and opportunities for commercialization of enhanced accident tolerant fuel for light water reactors: a utility-in-formed perspectively," IAEA TECDOC Series, 119, 2016.

[7] *B. Cheng, Y. J. Kim et P. Chou*, "Improving accident tolerance of nuclear fuel with coated Mo-alloy cladding," Nuclear Engineering Technology, Vol. 48, pag. 16-25, 2016.

[8] *R. Reback*, "Accident Tolerant Materials for Light Water Reactor Fuels," Elsevier, Chapter *2*, pag. 15-41, Chapter 2 2020.

[9] *K. Unocic, Y. Yukinori et B. Pint*, "Effect of Al and Cr Content on Air and Steam Oxidation of FeCrAl Alloys and Commercial APMT Alloy," Oxidation of Metals, Vol. 87, pag. 431-441, 2017.

[10] *B. Maier, H. Yeom, G. Johnson, T. Dabney, J. Walters, P. Xu, J. Romero, H. Shah et K. Sridharan*, "Development of cold spray chromium coatings for improved accident tolerant zirconium-alloy cladding," Journal of Nuclear Materials, Vol. 519, pag. 247–254, 2019.

[11] *H. Kim, I. Kim, Y. Jung, D. Park, J. Park et Y. Koo*, "Adhesion property and High-temperature oxidation behavior of Cr-coated Zircaloy-4 cladding tube prepared by 3D laser coating," Journal of Nuclear Materials, Vol. 465, pag. 531–539, 2015.

[12] *T. Wei, R. Zhang, H. Yang, H. Liu, S. Qiu, Y. Wang, P. Du, K. He, X. Hu et C. Dong*, "Microstructure, corrosion resistance and oxidation behavior of Cr-coatings on Zircaloy-4 prepared by vacuum arc plasma deposition," Science Direct, Vol. 158, 2019.

[13] *J. Park, H. Kim, J. Park, Y. Jung, D. Park et Y. Koo*, "High temperature steam-oxidation behavior of arc ion plated Cr coatings for accident tolerant fuel claddings," Surface and Coating Technology, Vol. 280, pag. 256–259, 2015.

[14] *C. Tang, M. Stueber, H. Seifert et M. Steinbrueck*, "Protective coatings on zirconium-based alloys as accident-tolerant fuel (ATF) claddings," Corrosion Reviews, Vol. 35, pag. 141–165, 2017.

[15] *K. Geelhood et W. Luscher*, "Degradation and failure phenomena of accident tolerant fuel concepts. Chromium coated zirconium alloy cladding," PNNL-28437, Washington, 2019.

[16] *C. Huan, W. Xiaoming et Z. Ruiqian*, "Application and Development Progress of Cr-Based Surface Coatings in Nuclear Fuel Element: I.Selection, Preparation, and Characteristics of Coating Materials," Coatings, Vol. 10, pag. 835, 2020.

[17] *J. Brachet, M. Le Saux, V. Lezaud-Chaillioux, M. Dumerval, Q. Houmaire, F. Lomello, F. Schuster, E. Monsifrot, J. Bischoff et E. Pouillier*, "Behavior under LOCA conditions of Enhanced Accident Tolerant Chromium Coated Zircaloy-4 Claddings," Top Fuel 2016, 11-15 September 2016.

[18] *E. Kashkarov, B. Afornu, D. Sidelev, M. Krinitcyn, V. Gouws et A. Lider*, "Recent advances in protective coatings for accident tolerant Zr-based fuel claddings," Coatings, Vol. 11 (5), pag. 557, 2021.

[19] *J. Brachet, I. Idarraga-Trujillo, M. Le Flem, M. .. Le Saux, V. Vandenberghe, S. Urvoy, E. Rouesne, T. Guilbert, C. Toffolon Masclet et M. Tupin*, "Early studies on Cr-Coated Zircaloy-4 as enhanced accident tolerant nuclear fuel claddings for light water reactors," Journal of Nuclear Materials, Vol. 517, pag. 268–285, 2019.

[20] *X. Wang, H. Guan, Y. Liao, M. Zhu, C. Xu, X. Jin, B. Liao, W. Xue, Y. Zhang et G. Bai*, "Enhancement of high temperature steam oxidation resistance of Zr–1Nb alloy with ZrO2/Cr bilayer coating," Corrosion Science, Vol. 187, 2021.

[21] *E. Kashkarov, D. Sidelev, M. Rombaeva, M. Syrtanov et G. Bleykher*, "Chromium coatings deposited by cooled and hot target magnetron sputtering for accident tolerant nuclear fuel claddings," Surface and Coating Technology, Vol. 389, 2020.

[22] *H. Yeom et K. Sridharan*, "Cold spray technology in nuclear energy applications: A review of recent advances," Annals of Nuclear Energy, Vol. 150, 2021.

[23] *K. Terrani*, "Accident tolerant fuel cladding development: Promise, status, and challenges," Journal of Nuclear Materials, Vol. 501, pag. 13-30, 2018.